Electronic Supplementary Information (ESI)

Overcoming ABCG2-mediated multidrug resistance by mineralized hyaluronan-drug nanocomplex

Wei Chen,[a] *Fang Wang,*[a] *Xu Zhang,*[a] *Jing Hu,*[b] *Xiaokun Wang,*[a] *Ke Yang,*[a] *Liyan Huang,*[a] *Meng Xu,*[a] *Qingshan Li*[b] *and Liwu Fu**[a]

[a]State Key Laboratory of Oncology in South China, Collaborative Innovation Center for Cancer Medicine, Cancer Center, Sun Yat-sen University, Guangzhou 510060, China. Email: Fulw@mail.sysu.edu.cn; Fax: +86-20-87343170; Tel: +86-20-87343164
[b]Department of Hematology, Guangzhou First People's Hospital, Guangzhou Medical University, Guangzhou 510180, China

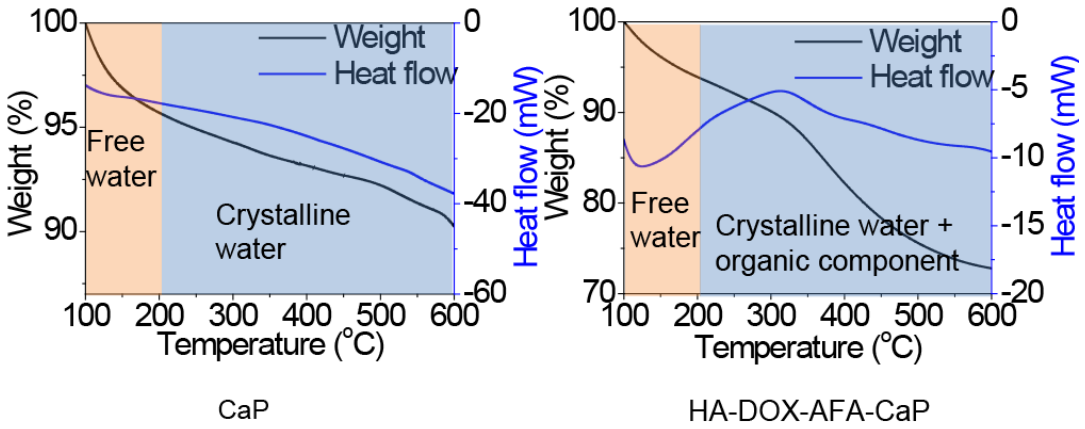

Fig. S1 The thermo gravimetric analysis and differential scanning calorimeter thermo examination (TGA/DSC) of native CaP nanoparticles and HA-DOX-AFA-CaP nanocomplex. Clearly, in CaP particle, the water (free water and crystalline water) account for around 10 wt% of total weight, which can roughly be used to estimate the water content in HA-DOX-AFA-CaP nanocomplex. Moreover, the content of inorganic core (CaP in amorphous state) in nanocomplex was about 74 wt% (final weight of HA-DOX-AFA-CaP after removing organic component and water) while organic component contributes around 16% of the total weight (100%-10%-74%=16%).

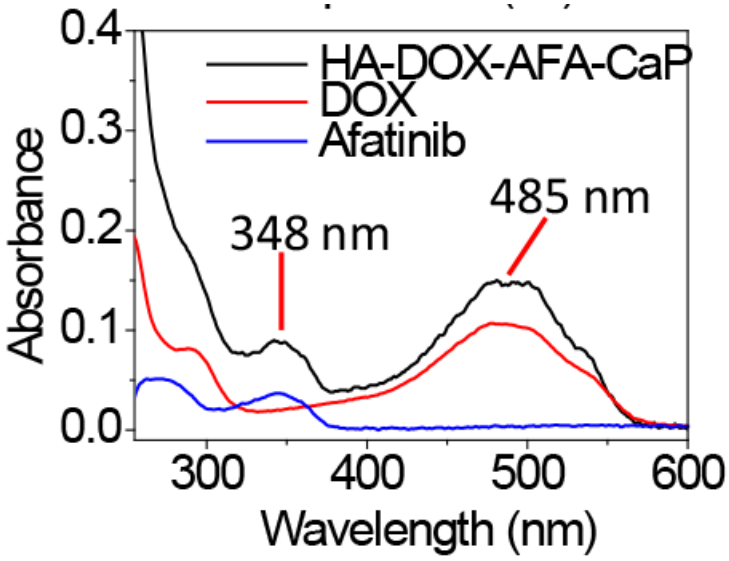

Fig. S2 Ultraviolet–Visible spectroscopy of free DOX, free AFA and HA-DOX-AFA-CaP nanocomplex.

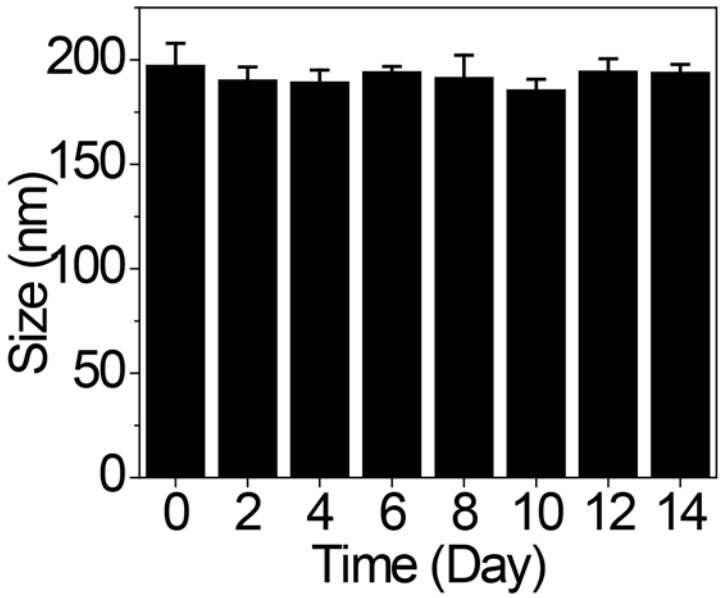

Fig. S3 The long-term stability of HA-DOX-AFA-CaP in DMEM with 10% FBS. The size showed nealy no change within 2 weeks.

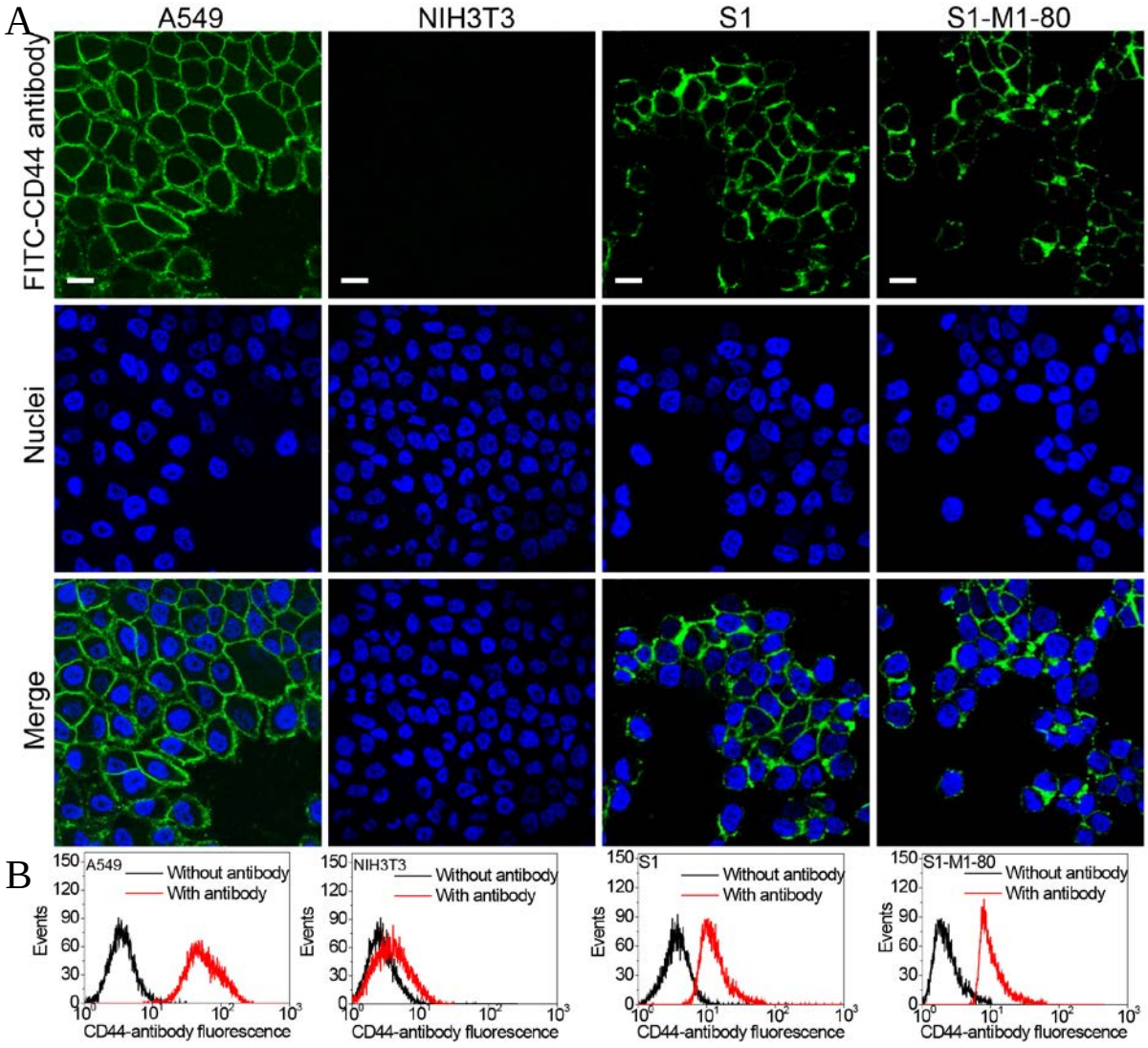

Fig. S4 (A) Expression level of CD44 on A549, NIH3T3, S1 and S-M1-80 cells characterized by confocal laser scanning microscope (CLSM) (bar = 15 μm). (B) Expression level of CD44 receptor on A549, NIH3T3, S1 and S-M1-80 cells characterized by flow cytometry analysis.

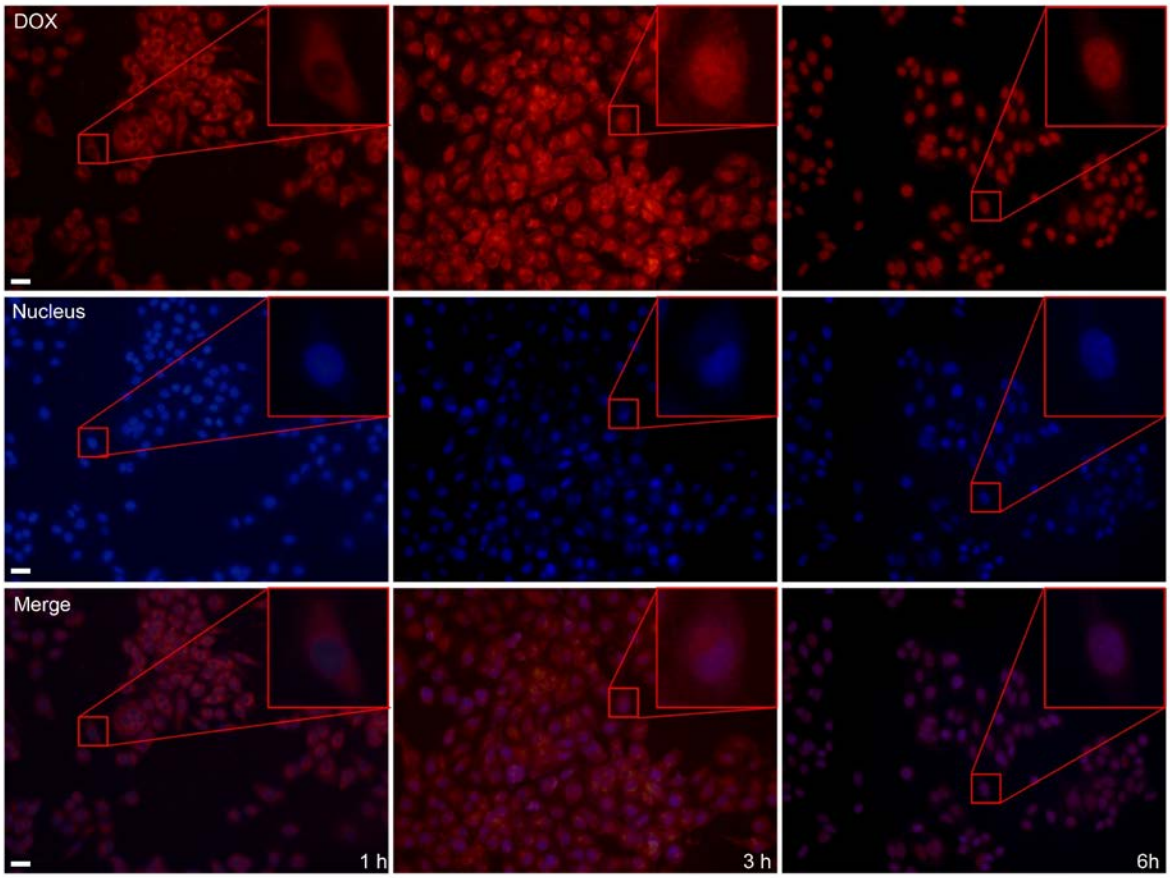

Fig. S5 Fluorescence images of HA-DOX-AFA-CaP particles inside S1-M1-80 cells at different time. From up to down: DOX emission (red) under 450-480 nm excitation; the nuclei (blue) stained by DAPI under 330-385 nm excitation; the merged image (bar = 20 μm). Results clearly reveal that nanocomplex entered into cells to release the drugs to continue reacting with nuclei.

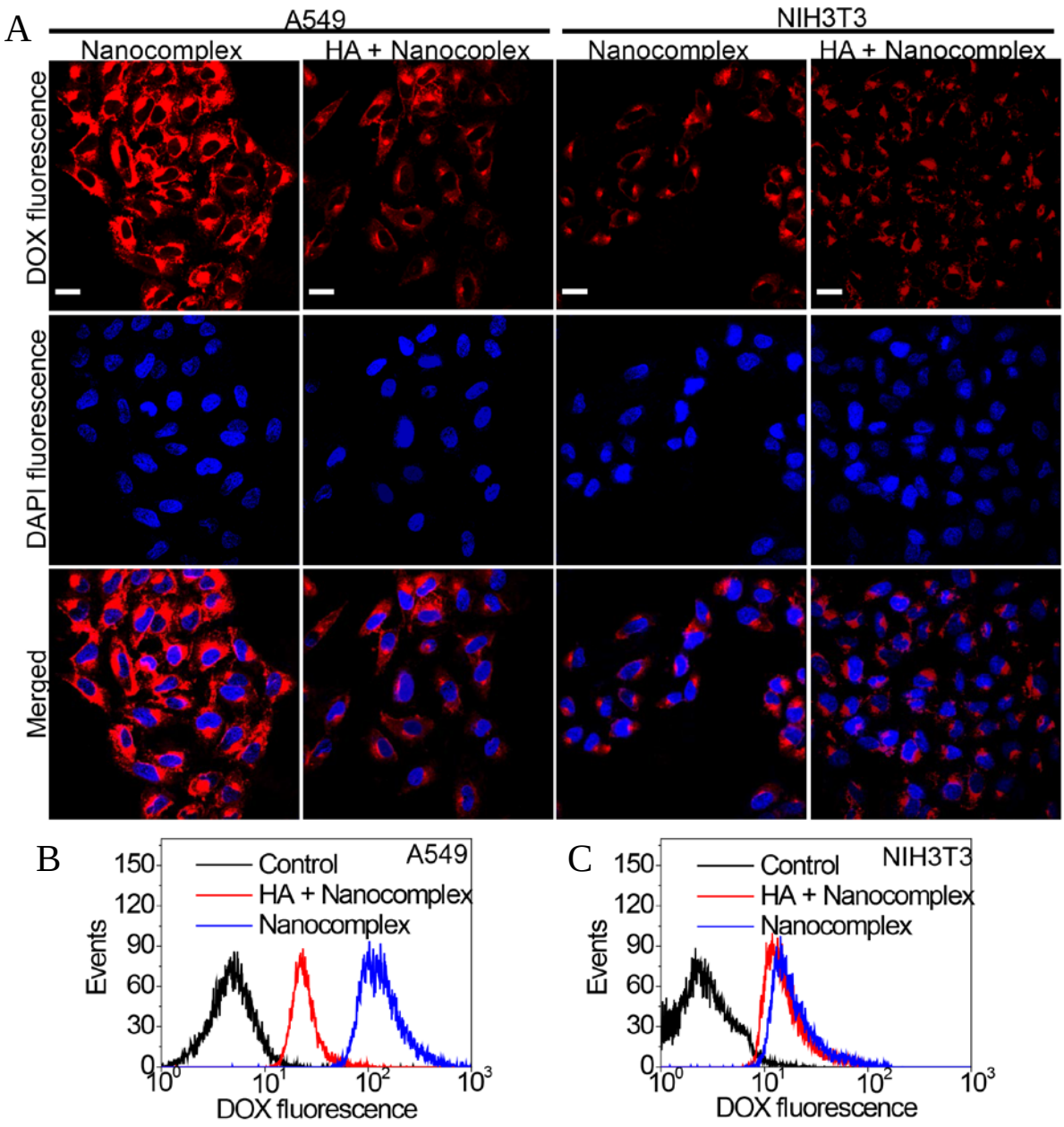

Fig. S6 The targeting ability of HA-based nanoparticles. (A) CLSM observation for the uptake of HA-DOX-AFA-CaP by A549 (left two columns) and NIH3T3 cells (right two columns) with or without HA pretreatment (bar = 15 μm). Flow cytometry analysis of competitive inhibition of HA to the uptake of HA-DOX-AFA-CaP particles in A549 cells (B) and NIH3T3 cells (C).

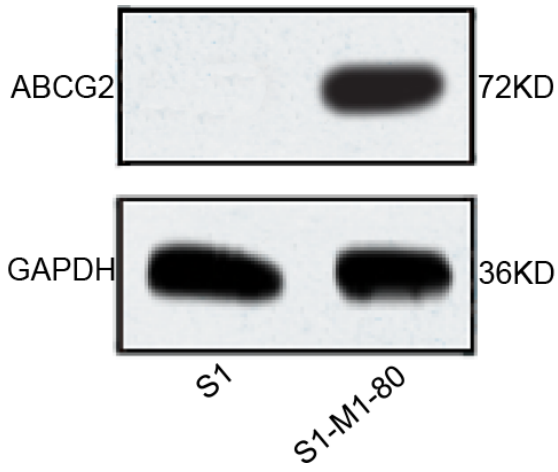

Fig. S7 Expression of ABCG2 protein in S1 and S1-M1-80 cells by western blot analysis.

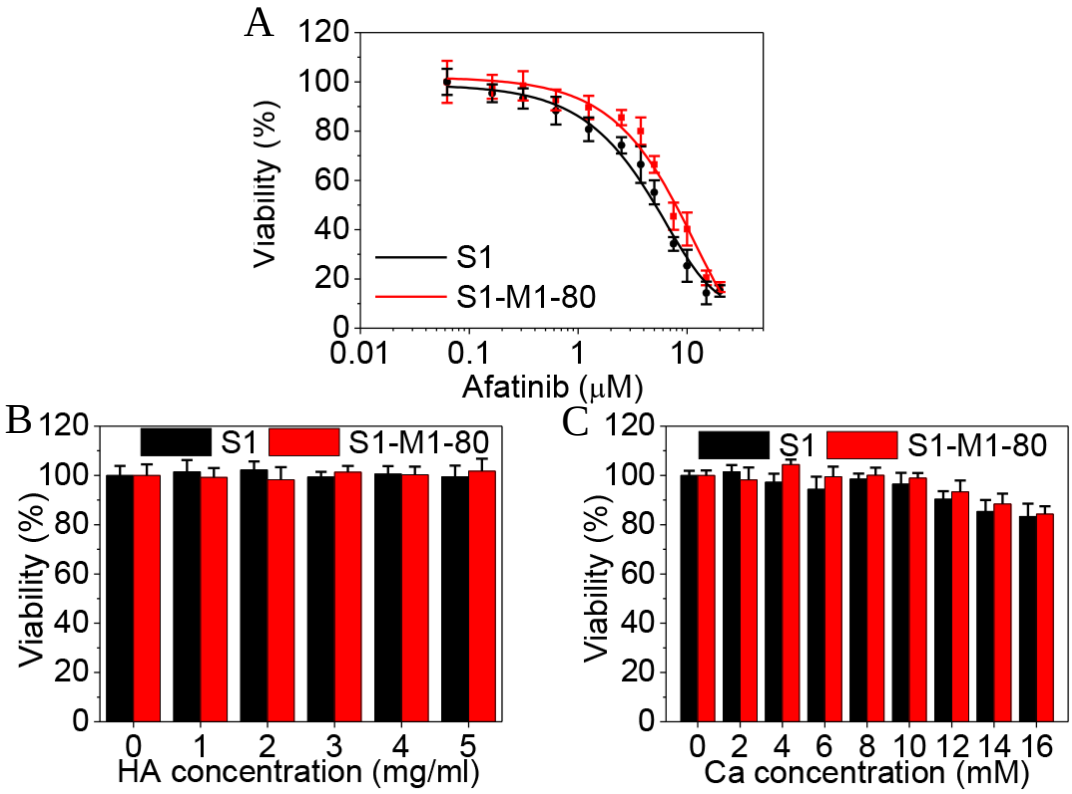

Fig. S8 In vitro cytotoxicity of (a) AFA, (b) HA and (c) CaP on S1 and S1-M1-80 cells.

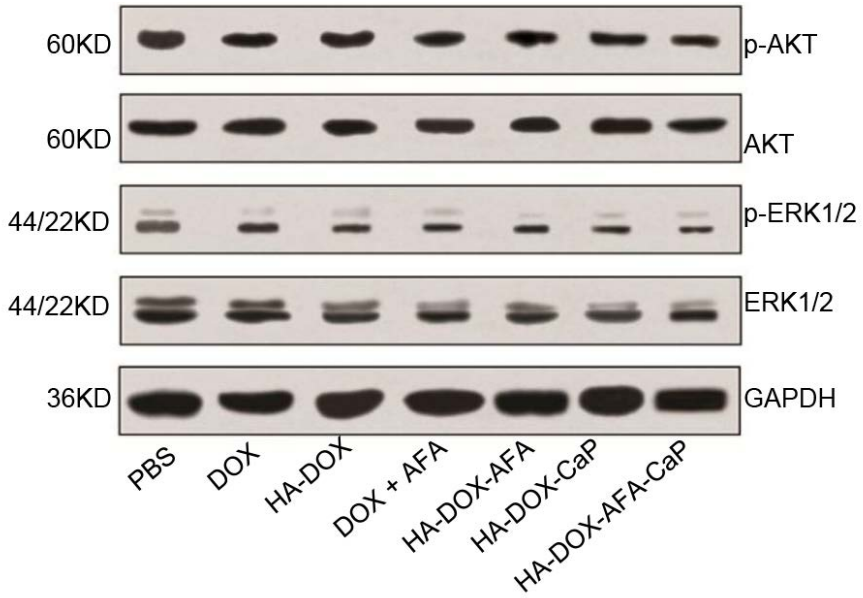

Fig. S9 Western blot analysis of influence of different treatments on the expression and phosphorylation of ERK1/2 and AKT in S1-M1-80 cells. Obviously, AFA-containing treatments showed ignorable effect on ERK1/2 and AKT signal pathways with low concentration (1.5 μM).